

No-insulation multi-width winding technique for high temperature superconducting magnet

Seungyong Hahn,^{a)} Youngjae Kim, Dong Keun Park, Kwangmin Kim, John P. Voccio, Juan Bascuán, and Yukikazu Iwasa

Francis Bitter Magnet Laboratory, Massachusetts Institute of Technology, 170 Albany Street, Cambridge, Massachusetts 02139, USA

(Received 5 June 2013; accepted 6 October 2013; published online 23 October 2013)

We present a *No-Insulation (NI) Multi-Width (MW)* winding technique for an HTS (high temperature superconductor) magnet consisting of double-pancake (DP) coils. The NI enables an HTS magnet self-protecting and the MW minimizes the detrimental anisotropy in current-carrying capacity of HTS tape by assigning tapes of multiple widths to DP coils within a stack, widest tape to the top and bottom sections and the narrowest in the midplane section. This paper presents fabrication and test results of an NI-MW HTS magnet and demonstrates the unique features of the NI-MW technique: self-protecting and enhanced field performance, unattainable with the conventional technique. © 2013 AIP Publishing LLC. [<http://dx.doi.org/10.1063/1.4826217>]

This paper presents a *No-Insulation Multi-Width (NI-MW)* winding technique applicable to 2G (2nd generation) HTS (high temperature superconductor) magnets assembled from stacks of double-pancake (DP) coils. We have already demonstrated experimentally that self-protecting HTS magnets are feasible with the NI technique, in which the key idea is to completely eliminate turn-to-turn insulation within the HTS DP windings.^{1,2} In the event of a quench, we confirmed that the magnet current in an NI winding automatically bypassed the quench spot through turn-to-turn contacts from its original spiral path and that the magnet remained stable even though its operating current was pushed to twice the magnet critical current.¹ Due to this self-protecting feature, an NI magnet requires a minimum amount of stabilizer, just enough for ease of splicing and handling.^{3–8} The absence of both turn-to-turn insulation and the extra stabilizer needed in its insulated (INS) counterpart makes the NI magnet highly compact and enhances its overall current density.^{9–18}

Commercial 2G conductor comes as tape with width/thickness ratio in a range of 5–40.^{19,20} Unlike a conventional assembly of DP coils, in which the DP coils are wound with the same-width 2G tape,^{21–23} in our MW technique, we place DP coils of the narrowest tape width in the magnet midplane section, placing DP coils of gradually wider tapes away from the midplane, with the widest-tape DP coils at the top and bottom sections, where the normal field that limits 2G tape performance is at its peak. This MW technique significantly enhances the overall current density of such a DP coil assembly at a given operating current.

On one hand, the NI technique enables an HTS magnet to be self-protecting and thus to operate at a high current density ($>150 \text{ kA/cm}^2$),² both features are not possible with the conventional HTS magnet. On the other hand, the MW technique is the most suitable and effective approach to “conductor-grade”²⁴ DP coils wound with highly anisotropic 2G HTS tape. A combination of NI and MW techniques (NI-MW) thus not only satisfies key operation requirements

in protection and stability but also enables HTS magnets to be highly compact, which will lead to significant reduction in magnet price, one of the decisive factors in the marketplace.

To demonstrate the NI-MW concept, we have designed and constructed a test NI-MW magnet as seen in Fig. 1(a). It consists of a stack of seven DP coils wound with “bare (no copper stabilizer)” 2G conductor, manufactured by AMSC without any turn-to-turn insulation (NI technique). The original conductor was 46-mm wide and then was mechanically slit to have a target width. The conductor width is 2.5 mm for the center DP coil (DP4 in Fig. 1) and increases up to 4.0 mm for the top and bottom DP coils (DP1 and DP7). As a result, this MW magnet generates 22% greater field than its single-width (SW) counterpart with the same overall dimensions (inner diameter, outer diameter, and height) as those of the SW magnet at a given operating current. Fig. 1(b) is a picture of DP4 and Table I presents key magnet parameters of the test magnet.

Two tests were performed in a bath of liquid nitrogen at 77 K: (1) charge-discharge test to compare spatial and temporal field performances of the NI-MW magnet with those of

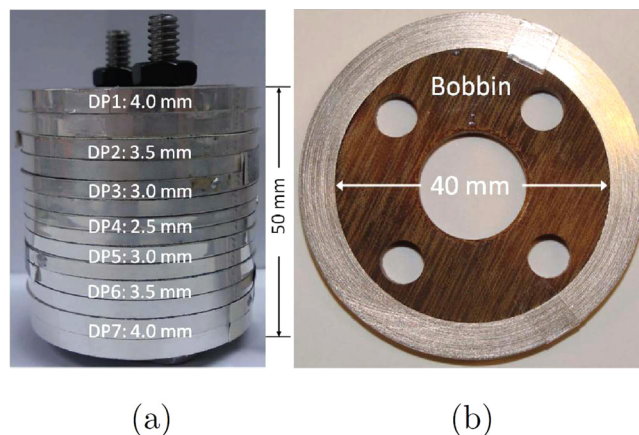


FIG. 1. (a) Picture of the test NI-MW magnet (7 DP coils); (b) picture of DP4 (2.5 mm tape width).

^{a)} Author to whom correspondence should be addressed. Electronic mail: syhahn@mit.edu

TABLE I. Key parameters of the test NI-MW magnet.

Parameters	Values
HTS wire width [mm]	2.5; 3.0; 3.5; 4.0
HTS wire thickness [mm]	0.08
Stabilizer	n/a
Winding inner diameter [mm]	40
Winding outer diameter [mm]	50
Overall height [mm]	50
Number of DP coils	7
Turn per DP	120
Critical current at 77 K [A]	25
Charging time constant [s]	0.81
Magnet constant [mT/A]	16.5
Inductance [mH]	18.9

its INS and SW counterparts; and (2) over-current test to demonstrate the superior stability and the self-protecting feature of the NI-MW magnet.

The NI-MW magnet was charged to 20 A (80% of the magnet critical current, 25 A), and the axial fields were measured along the magnet axis. Fig. 2 compares the measured fields (squares) with calculated ones of its INS-MW (lines) and INS-SW (dashes) counterparts. For ease of comparison, the inner diameter, outer diameter, and overall height of INS-MW and INS-SW magnets used in calculation are set to be identical to those of the NI-MW magnet; the insulation thickness of the INS-MW magnet is assumed to be negligible and the INS-SW magnet is assumed to have a uniform overall current density equivalent to that of DP1 or DP7 in the test magnet. The results show that the spatial field performance of the NI magnet is virtually identical to that of its INS counterpart and that the MW version generates 22% more field than its SW counterpart.

Fig. 3 shows power supply current and axial center field from a 20-A charge-discharge test; squares are for power supply current; circles for measured fields; triangles for calculated fields by a proposed circuit model in Fig. 4. The inset, an enlarged view of the plots near the end of charging, reveals a discernible delay (~ 1 s) between current and corresponding field. The time constants, 0.81 s (measured) and

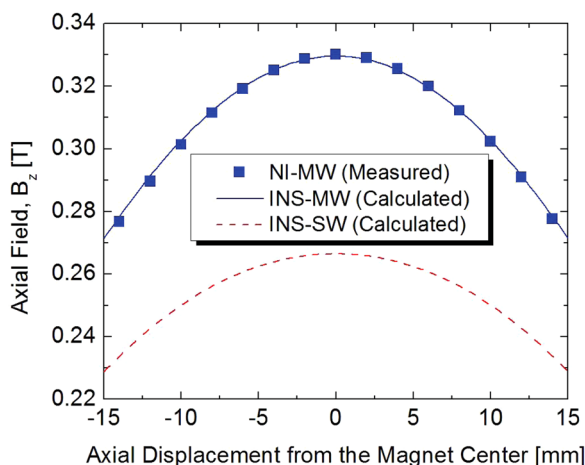


FIG. 2. Axial fields along the magnet axis; NI-MW: no-insulation multi-width; INS-MW: insulated multi-width; INS-SW: insulated single-width.

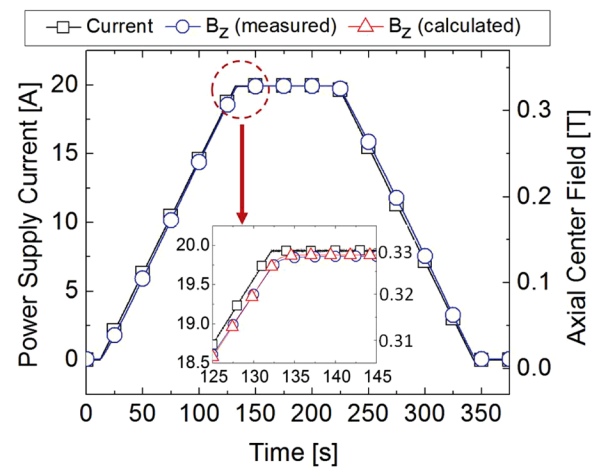


FIG. 3. Charge-discharge test results. The inset is an enlarged view of the dashed circle.

0.79 s (calculated), agree well. The results validate the proposed circuit model to accurately characterize the electrical responses of an NI-MW magnet.

In the over-current test, the NI-MW magnet was charged up to 60 A at a rate of 0.5 A/min, a typical charging rate for actual nuclear magnetic resonance magnets, which are one of major target applications of the NI-MW technique. Fig. 5 presents the test results: squares, circles, and triangles are for power supply current, axial center field, and terminal voltage, respectively. The axial field is proportional to the power supply current up to point “A” in Fig. 5 when the power supply current reaches the magnet critical current, 25 A. After “A,” the axial field starts saturating because a portion of the power supply current begins automatically bypassing through turn-to-turn contacts (R_R in Fig. 4) from its original spiral path. At “B,” the axial field reaches its peak and starts decreasing. Although at “C,” the power supply current, 60 A, was 2.2 times larger than the magnet critical current, this NI-MW magnet had operated stably without overheating for the next ~ 20 min. The test results were repeatable and the magnet was not damaged. In a separate test performed under the same cryogenic condition, i.e., in a bath of liquid nitrogen at

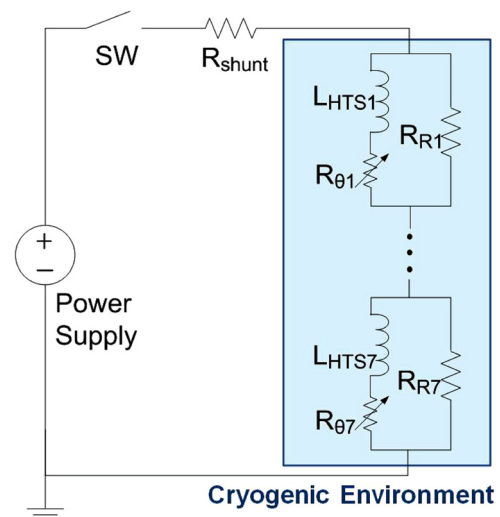


FIG. 4. Circuit diagram of the test setup with an equivalent circuit of the test NI-MW magnet in the shaded box.

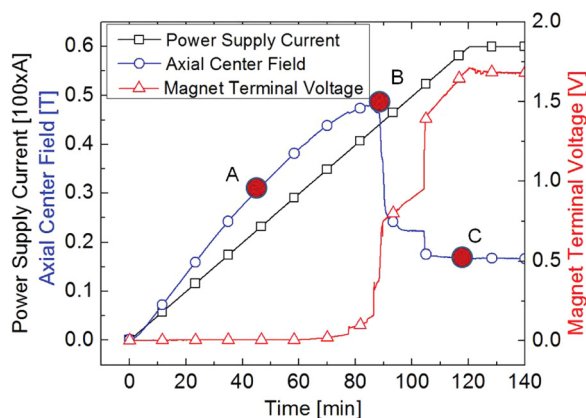


FIG. 5. Over-current test results of the test NI-MW magnet.

77 K, the 2.5-mm wide conductor was burned at 43 A, which demonstrates the *self-protecting* feature of the NI magnet.

Without turn-to-turn insulation, this test NI-MW magnet was successfully charged and discharged; its spatial field distribution under steady state was virtually identical to that of its INS counterpart. The measured charging time constant, 0.81 s, is consistent with the simulated one from the proposed equivalent circuit model.

With a single 2.5-mm DP4, the test NI-MW magnet generated 22% more field than its SW counterpart. If more 2.5-mm DP coils were used at the center, the field would increase by up to 1.6 times (4.0 mm/2.5 mm). With wider conductors at the top and bottom of the magnet, the field will increase further because the magnet can operate at a higher current.

In conclusion, we presented a NI DP winding technique with MW 2G HTS that results in a compact and self-protecting HTS winding. NI coils operate even more stable than their INS counterparts. Furthermore, the MW technique significantly enhances, for a given operating current, the overall current density of a magnet assembled from DP coils. Although the NI and MW techniques can be separately used, a combination of these two techniques makes these coils exceptionally “high-performing.” A test NI-MW magnet was constructed and operated in a bath of liquid nitrogen at 77 K to confirm its superior performance with regards to protection and field generation over its conventional insulated or single-width counterparts. The results have demonstrated that the NI-MW technique is indeed applicable and highly beneficial to most direct current HTS magnets.

This work was supported by the National Institute of Biomedical Imaging and Bioengineering of the National Institutes of Health under Award No. R21EB013764.

- ¹S. Hahn, D. K. Park, J. Bascuñán, and Y. Iwasa, *IEEE Trans. Appl. Supercond.* **21**, 1592 (2011).
- ²S. Hahn, D. K. Park, J. Voccio, J. Bascuñán, and Y. Iwasa, *IEEE Trans. Appl. Supercond.* **22**, 4302405 (2012).
- ³K. Kawai, S. Ito, Y. Seino, N. Yanagi, H. Tamura, A. Sagara, and H. Hashizume, *IEEE Trans. Appl. Supercond.* **23**, 4801704 (2013).
- ⁴C. A. Baldan, U. R. Oliveira, A. A. Bernardes, V. P. Oliveira, C. Y. Shigue, and E. Ruppert, *J. Supercond. Novel Magn.* **26**, 2089 (2013).
- ⁵Y. Kim, J. Bascuñán, T. Lecrevisse, S. Hahn, J. Voccio, D. K. Park, and Y. Iwasa, *IEEE Trans. Appl. Supercond.* **23**, 6800704 (2013).
- ⁶T. Lecrevisse, J. Gheller, O. Louchart, J. Rey, and P. Tixador, *Phys. Proc.* **36**, 681 (2012).
- ⁷K. S. Chang, H. C. Jo, Y. J. Kim, M. C. Ahn, and T. K. Ko, *IEEE Trans. Appl. Supercond.* **21**, 3005 (2011).
- ⁸J. Lu, K. Han, W. R. Sheppard, Y. L. Viouchkov, K. W. Pickard, and W. D. Markiewicz, *IEEE Trans. Appl. Supercond.* **21**, 3009 (2011).
- ⁹X. Wang, S. Hahn, Y. Kim, J. Bascuñán, J. Voccio, H. Lee, and Y. Iwasa, *Supercond. Sci. Technol.* **26**, 035012 (2013).
- ¹⁰Y. H. Choi, S. Hahn, J. B. Song, D. G. Yang, and H. G. Lee, *Supercond. Sci. Technol.* **24**, 125013 (2011).
- ¹¹Y. S. Choi, D. L. Kim, and S. Hahn, *IEEE Trans. Appl. Supercond.* **21**, 1644 (2011).
- ¹²Y.-G. Kim, S. Hahn, K. L. Kim, O. J. Kwon, and H. Lee, *IEEE Trans. Appl. Supercond.* **22**, 5200604 (2012).
- ¹³S. Choi, H. C. Jo, Y. J. Hwang, S. Hahn, and T. K. Ko, *IEEE Trans. Appl. Supercond.* **22**, 4904004 (2012).
- ¹⁴Y. H. Choi, K. L. Kim, O. J. Kwon, D. H. Kang, J. S. Kang, T. K. Ko, and H. G. Lee, *Supercond. Sci. Technol.* **25**, 105001 (2012).
- ¹⁵S. B. Kim, A. Saito, T. Kaneko, J. H. Joo, J. M. Jo, Y. J. Han, and H. S. Jeong, *IEEE Trans. Appl. Supercond.* **22**, 4701504 (2012).
- ¹⁶S. Hahn, Y. Kim, J. Ling, J. Voccio, D. K. Park, J. Bascuñán, H.-J. Shin, H. Lee, and Y. Iwasa, *IEEE Trans. Appl. Supercond.* **23**, 4601705 (2013).
- ¹⁷S. Yoon, K. Cheon, H. Lee, S. Moon, I. Ham, Y. Kim, S. Park, H. Joo, K. Choi, and G.-W. Hong, *IEEE Trans. Appl. Supercond.* **23**, 4600604 (2013).
- ¹⁸S. B. Kim, T. Kaneko, H. Kajikawa, J. H. Joo, J.-M. Jo, Y.-J. Han, and H.-S. Jeong, *IEEE Trans. Appl. Supercond.* **23**, 7100204 (2013).
- ¹⁹M. W. Rupich, X. Li, S. Sathyamurthy, C. L. H. Thieme, K. DeMoranville, J. Gannon, and S. Fleshler, *IEEE Trans. Appl. Supercond.* **23**, 6601205 (2013).
- ²⁰W. H. Fietz, C. Barth, S. Drotziger, W. Goldacker, R. Heller, S. I. Schlachter, and K.-P. Weiss, *Fusion Eng. Des.* **88**, 440 (2013).
- ²¹M. Daibo, S. Fujita, M. Haraguchi, Y. Iijima, M. Itoh, and T. Saitho, *IEEE Trans. Appl. Supercond.* **23**, 4602004 (2013).
- ²²S. Hahn, J. Bascuñán, H. Lee, E. S. Bobrov, W. Kim, M. C. Ahn, and Y. Iwasa, *J. Appl. Phys.* **105**, 024501 (2009).
- ²³B. J. Parkinson, R. Slade, M. J. D. Mallett, and V. Chamritski, *IEEE Trans. Appl. Supercond.* **23**, 4400405 (2013).
- ²⁴A. Ishiyama, M. Yanai, T. Morisaki, H. Ueda, S. Akita, S. Kouso, Y. Tatsuta, H. Abe, and K. Tasaki, *IEEE Trans. Appl. Supercond.* **15**, 1879 (2005).